

Wind-Tunnel Test of the S814 Thick-Root Airfoil

Dan M. Somers
James L. Tangler

*Prepared for
Fourteenth ASME-ETCE
Wind Energy Symposium
January 29–February 1, 1995
Houston, Texas*



National Renewable Energy Laboratory
1617 Cole Boulevard
Golden, Colorado 80401-3393
A national laboratory of the U.S. Department of Energy
Managed by Midwest Research Institute
for the U.S. Department of Energy
under contract No. DE-AC36-83CH10093

Prepared under Task No. WE518320

January 1995

NOTICE

This report was prepared as an account of work sponsored by an agency of the United States government. Neither the United States government nor any agency thereof, nor any of their employees, makes any warranty, express or implied, or assumes any legal liability or responsibility for the accuracy, completeness, or usefulness of any information, apparatus, product, or process disclosed, or represents that its use would not infringe privately owned rights. Reference herein to any specific commercial product, process, or service by trade name, trademark, manufacturer, or otherwise does not necessarily constitute or imply its endorsement, recommendation, or favoring by the United States government or any agency thereof. The views and opinions of authors expressed herein do not necessarily state or reflect those of the United States government or any agency thereof.

Available to DOE and DOE contractors from:
Office of Scientific and Technical Information (OSTI)
P.O. Box 62
Oak Ridge, TN 37831
Prices available by calling (615) 576-8401

Available to the public from:
National Technical Information Service (NTIS)
U.S. Department of Commerce
5285 Port Royal Road
Springfield, VA 22161
(703) 487-4650



WIND-TUNNEL TEST OF THE S814 THICK ROOT AIRFOIL

Dan M. Somers
Airfoils, Incorporated
601 Cricklewood Dr.
State College, PA 16803

James L. Tangler
National Renewable Energy Laboratory
1617 Cole Boulevard
Golden, CO 80401

ABSTRACT

The objective of this wind-tunnel test was to verify the predictions of the Eppler Airfoil Design and Analysis Code for a very thick airfoil having a high maximum lift coefficient ($c_{l,max}$) designed to be largely insensitive to leading edge roughness effects. The 24-percent-thick S814 airfoil was designed with these characteristics to accommodate aerodynamic and structural considerations for the root region of a wind-turbine blade. In addition, the airfoil's maximum lift-to-drag ratio was designed to occur at a high lift coefficient. To accomplish the objective, a two-dimensional wind-tunnel test of the S814 thick root airfoil was conducted in January 1994 in the low-turbulence wind tunnel of the Delft University of Technology Low Speed Laboratory. Data were obtained for transition-free and transition-fixed conditions at Reynolds numbers of 0.7, 1.0, 1.5, 2.0, and 3.0×10^6 . For the design Reynolds numbers of 1.5×10^6 , the transition-free $c_{l,max}$ is 1.3 which satisfies the design specification. However, this value is significantly lower than the predicted $c_{l,max}$ of almost 1.6. With transition-fixed at the airfoil leading edge, the $c_{l,max}$ is 1.2. The difference in $c_{l,max}$ between the transition-free and transition-fixed conditions demonstrates the airfoil's minimal sensitivity to roughness effects. The S814 root airfoil was designed to complement existing NREL low $c_{l,max}$ tip-region airfoils for rotor blades 10 to 15 meters in length.

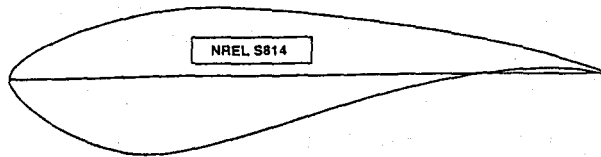
INTRODUCTION

Verification of the Eppler Airfoil Design and Analysis Code (Eppler, 1994) has been the goal of several NREL - sponsored, comprehensive, two-dimensional tests in the low-turbulence wind tunnel of the Delft University of Technology Low Speed Laboratory, the Netherlands. Initial verification of the code was based on data acquired for low maximum lift coefficient ($c_{l,max}$) airfoils of the thin and thick airfoil families. The first of these tests was conducted in 1985 upon completion of the design effort for a thin airfoil family for stall-regulated rotors. The primary airfoil of this family, the S805, was extensively tested (Somers, 1988) and the results showed that the Eppler Airfoil Design and Analysis Code predicted all the section characteristics well except the profile drag. The profile drag was underpredicted as a result of underestimating the significance of the laminar separation bubbles, through which the laminar flow on both the

upper and lower surfaces transitions to turbulent flow. The design of the subsequent thick airfoil family included an adjustment to the design process that accounted for this bias error. In 1986, this adjustment was verified in a wind-tunnel test of the S809, the primary airfoil, of this family (Somers, 1989). Through these tests, the Eppler Airfoil Design and Analysis Code was "calibrated" so future airfoils, of moderate thickness, could be designed with greater confidence. For wind-turbine blades, moderate thickness airfoils are typically used for the outboard portion of the blade.

For the root region of a wind-turbine blade, structural and dynamic considerations require greater airfoil thickness. However, for thicknesses over 26-percent chord, it is difficult to design desirable performance characteristics into an airfoil. These characteristics include a high $c_{l,max}$ that is largely insensitive to roughness effects along with low profile drag over a wide range of lift coefficients. Also, the maximum lift-to-drag ratio must occur at a high lift coefficient and the pitching moment should not be excessive. In the case of stall-regulated blades, it is desirable to transition from the high $c_{l,max}$ of the root airfoil to a low $c_{l,max}$ for the tip-region airfoil. In 1992, these guidelines were used for the design of the 24-percent-thick S814 airfoil (Somers, 1992). Its shape and specifications are shown in Figure 1. A roughness insensitive, maximum lift coefficient of at least 1.3 for a Reynolds number of 1.5×10^6 was the goal for the blade root region. Low profile-drag coefficients were desired over the range of lift coefficients from 0.6 to 1.2 at the design Reynolds number. The zero-lift pitching moment coefficient was to be no more negative than -0.15.

To verify the predictions of the Eppler Airfoil Design and Analysis Code for extra thick, root airfoils having a high $c_{l,max}$ such as the S814 airfoil, a third, highly accurate, wind-tunnel test was conducted. Based on the need for a well-documented, highly accurate, low-turbulence wind tunnel, the Delft University of Technology Low Speed Laboratory tunnel was selected for this test. Comprehensive testing was conducted in January 1994 for both smooth and rough surface conditions (Somers, 1994). The resulting data were used to identify discrepancies between predicted and measured airfoil characteristics and to compare with the previously acquired S805 and S809 data. These efforts have helped to provide further validation and improvements to the Eppler Airfoil Design and Analysis Code.



Design Specifications

Airfoil	t/R	Reynolds Number	t/c	$C_{l,max}$	$C_{d,min}$	$C_{m,0}$
S814	0.40	1.5×10^6	0.240	1.3	0.012	-0.15

FIGURE 1. S814 AIRFOIL SHAPE AND PERFORMANCE SPECIFICATIONS

WIND-TUNNEL TESTING

The low-turbulence wind tunnel of the Delft University of Technology Low Speed Laboratory, is a closed-throat, single-return, atmospheric tunnel. The octagonal test section is 1800 mm (70.9 in.) wide by 1250 mm (49.2 in.) high. The turbulence level in the test section varies from 0.02 percent at 10 m/s (30 ft/s) to 0.04 percent at 60 m/s (200 ft/s). Measurements of the basic tunnel pressures, the pressures on the model, and the wake-rake pressures were made using a multitube manometer which was read automatically using fiber-optic photoelectric cells. An electronic data-acquisition system was used to obtain and record data.

The composite, wind-tunnel model had a chord of 650 mm (25.6 in.) and a span of 1248 mm (49.1 in.). Upper- and lower-surface orifices were 0.40 mm (0.016 in.) in diameter and located to one side of the midspan in a staggered row. Heating elements for infrared flow visualization were bonded into the upper and lower shells. The surface of the model consisted of polyester gelcoat which had been sanded and polished to ensure an aerodynamically smooth finish. The measured model contour was within 0.07 mm (0.003 in.) of the prescribed shape.

The model was tested at Reynolds numbers of 0.7, 1.0, 1.5, 2.0, and 3.0×10^6 with transition free (smooth) and with transition fixed by roughness at 2-percent chord on the upper surface and 10-percent chord on the lower surface. The grit roughness was sized using the method of Braslow (1958) and sparsely distributed along 3-mm (0.1-in.) wide strips applied to the model with lacquer. The model was also tested with more severe roughness developed for field testing of wind-turbine blades (Tangler, 1990). This granular roughness varied in size from 0.38 mm (0.015 in.) to 0.64 mm (0.025 in.) and was sparsely distributed onto double-coated adhesive tape 51-mm (2.0-in.) wide and 0.05-mm (0.002-in.) thick. The centerline of the tape was aligned with 2-percent chord on the upper surface and 10-percent chord on the lower surface. This method results in no grit being present around the leading edge stagnation point where the boundary layer is very stable with minimal sensitivity to roughness. For several test runs, the model surfaces were coated with oil to determine the location, as well as the nature, of the boundary-layer transition from laminar to turbulent flow. Transition was also located using infrared flow visualization by a method discussed by Quast (1987).

TEST RESULTS

The measured pressure distributions at various angles of attack for a Reynolds number of 1.5×10^6 and a Mach number of 0.10 with transition free are shown in Figure 2. At an angle of attack of -0.05° , a laminar separation bubble is evident on the upper surface around 45-percent chord and on the lower surface around 30-percent chord. As the angle of attack is increased, the bubble on the upper surface moves

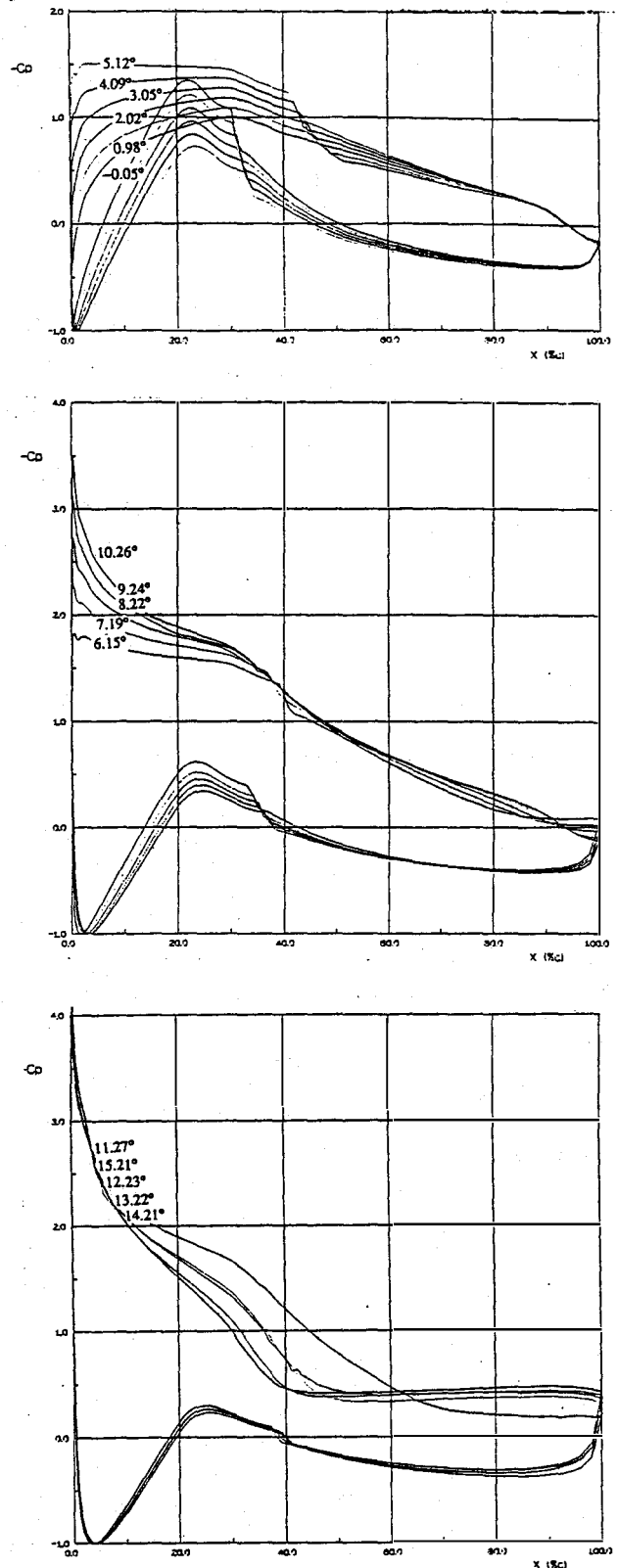


FIGURE 2. MEASURED PRESSURE DISTRIBUTIONS FOR S814 AIRFOIL WITH TRANSITION FREE (REYNOLDS NUMBER 1.5×10^6)

slowly forward and decreases in length; whereas, the bubble on the lower surface moves slowly aft and increases slightly in length. At an angle of attack of 7.19° , which corresponds to the upper limit of the low-drag range, the bubble on the upper surface has almost disappeared. As the angle of attack is increased further, turbulent, trailing-edge separation occurs on the upper surface. The amount of separation increases slowly with increasing angle of attack. The maximum lift coefficient occurs at an angle of attack just beyond 10.26° . As the angle of attack is increased further, the separation point moves rapidly forward to about 40-percent chord and then slowly migrates further forward (not shown).

The mechanism for the transition from laminar to turbulent flow on both surfaces is a laminar separation bubble. The variation of transition location with lift coefficient, as determined by infrared flow visualization, is shown in Figure 3 for lift coefficients for which there exists laminar separation bubbles. The transition location measured corresponds to the turbulent-reattachment point since the laminar separation cannot be detected using this technique. The transition location on the upper surface moves slightly forward with increasing Reynolds number; whereas, the lower-surface transition location varies little with Reynolds numbers. The application of turbulators (Somers, 1989) to the S8 14 for eliminating the laminar separation bubbles on the upper and lower surfaces did not lower the drag coefficients, even for the lowest Reynolds number of 0.7×10^6 . These results confirm the achievement of the design goal to eliminate significant (drag-producing) laminar separation bubbles through the incorporation of transition ramps in the pressure distributions.

The section characteristics with transition free and transition fixed are shown in Figure 4. For the design Reynolds number of 1.5×10^6 with transition free, the maximum lift coefficient is 1.3, which meets the design objective. Low drag coefficients are exhibited over the range of lift coefficients from about -0.6 to about 1.2. Thus, the lower limit of the low-drag range is well below the design objective and the upper

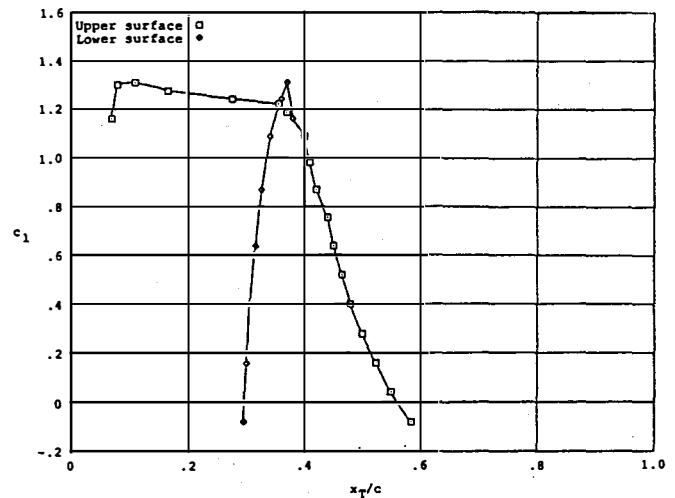


FIGURE 3. MEASURED TRANSITION LOCATION FOR S8 14 AIRFOIL (REYNOLDS NUMBER 1.5×10^6)

limit meets the design objective. The drag coefficient at the specified lower limit of the low-drag range ($c_l = 0.6$) is 0.0097. The zero-lift pitching-moment coefficient is -0.137 which is slightly less negative than the design constraint.

With transition fixed, the lift-curve slope and the pitching-moment coefficients decrease in magnitude. These results are caused primarily by the boundary-layer displacement effect which decambers the airfoil as a result of the displacement thickness being greater for the transition-fixed condition than for the transition-free condition. In addition, the lift-curve slope decreases with transition fixed because the roughness induces earlier trailing-edge separation. The maximum lift

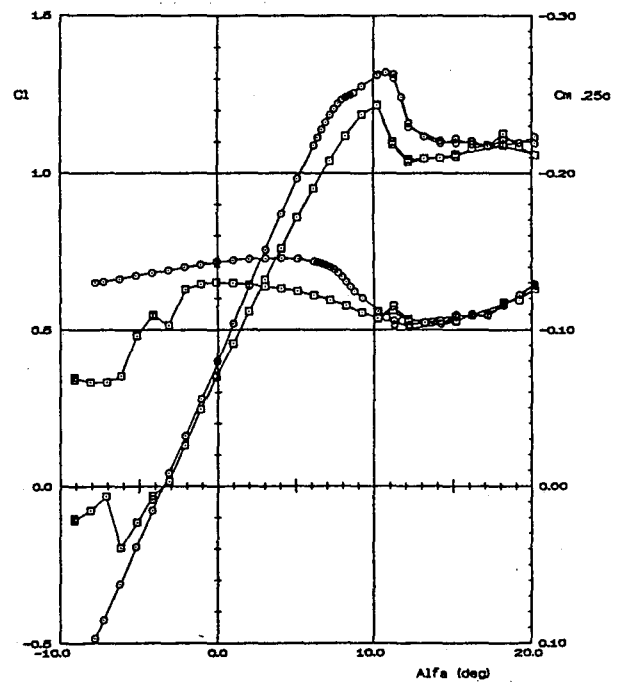
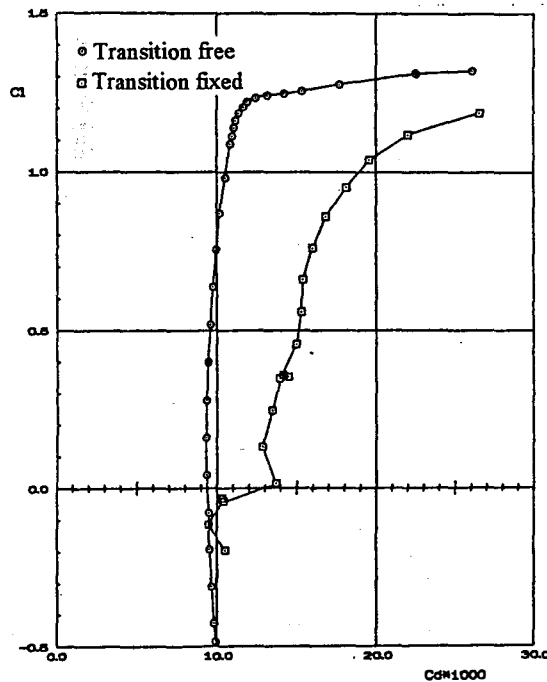


FIGURE 4. MEASURED SECTION CHARACTERISTICS OF S814 AIRFOIL TRANSITION FREE AND TRANSITION FIXED (REYNOLDS NUMBER 1.5×10^6)

coefficient for the design Reynolds number of 1.5×10^6 is 1.2, a reduction of 8 percent from that for the transition-free condition. The drag coefficients increases by over 50 percent as a result of fixing transition. In general, the lift-curve slope, the maximum lift coefficient, and the zero-lift pitching-moment coefficient increase in magnitude with increasing Reynolds number while the upper limit of the low-drag range and the drag coefficients decrease. The zero-lift angle of attack, -3.5° , is essentially unaffected by Reynolds number. The stall characteristics become less docile with increasing Reynolds number.

The effect of severe roughness (Tangler, 1990) on the section characteristics, relative to the transition-free case, is shown in Figure 5. With severe roughness, the lift curve slope and the pitching moment coefficient undergo a further decrease in magnitude relative to the transition-fixed case of Figure 4. Additional boundary-layer displacement results in more decambering of the airfoil. The maximum lift coefficient drops to 1.01, a reduction of 23 percent from that of the transition-free case. As expected, the severe roughness leads to over a 60 percent increase in the drag coefficient. The effect of fixed transition and severe roughness on the maximum lift coefficient is summarized in Figure 6. In general, the effect of fixing transition decreases with increasing Reynolds number; whereas, the effect of the severe roughness is essentially constant. It should be remembered that the effects of roughness are related to the ratio of the roughness height to the airfoil chord. Therefore, the effects of this roughness may be exaggerated because the chord of the wind-tunnel model is smaller than the chord of the wind-turbine blade at the corresponding blade radial station.

The comparison of theoretical and experimental section characteristics with transition free is shown in Figure 7. In general, the magnitudes of the zero-lift angle of attack, the upper limit of the low-drag range, and the pitching-moment coefficients are overpredicted. The lift-curve slope is slightly underpredicted and the maximum lift coefficient is significantly overpredicted. The drag

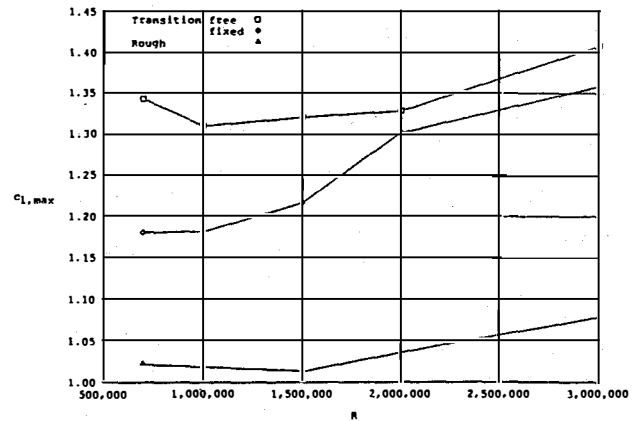


FIGURE 6. EFFECT OF ROUGHNESS ON MAXIMUM LIFT COEFFICIENT AS A FUNCTION OF REYNOLDS NUMBER

coefficients are predicted relatively accurately in the low-drag range. The overprediction of the upper limit of the low-drag range and the pitching-moment coefficients is typical of the method and accounted for in the design of the airfoil. The significant overprediction of the maximum lift coefficient is not typical. The accurate prediction of the drag coefficients further confirms the achievement of the goal to eliminate significant laminar separation bubbles.

Comparisons of the experimental section characteristics of the S814 airfoil with the NACA 4424 and 23024 airfoils (Abbott, 1945) are shown in Figures 8 and 9, respectively, with transition free for a Reynolds number of 3.0×10^6 . The S814 airfoil achieves a higher maximum lift coefficient and exhibits lower drag coefficients than do the NACA airfoils. The S814 airfoil also produces more negative pitching-

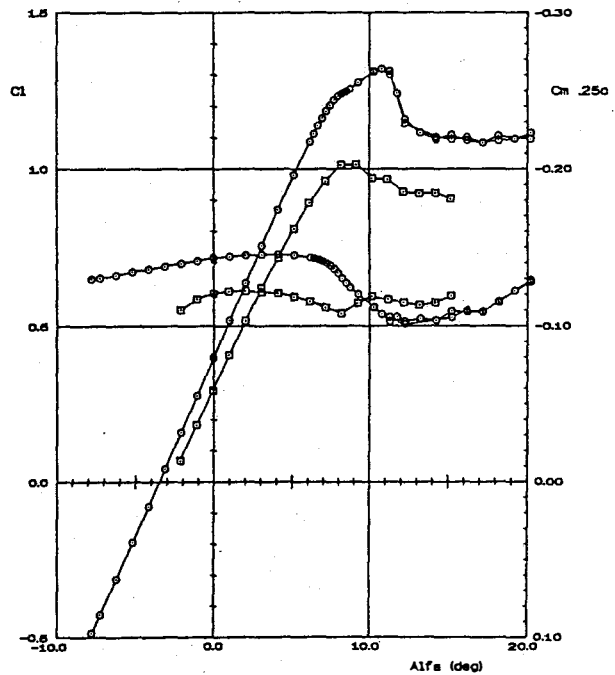
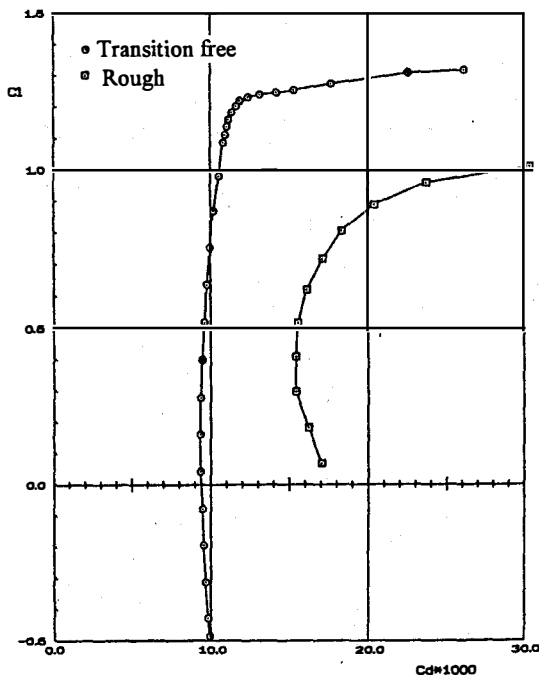


FIGURE 5. MEASURED SECTION CHARACTERISTICS OF S814 AIRFOIL TRANSITION FREE AND SEVERE ROUGHNESS (REYNOLDS NUMBER 1.5×10^6)

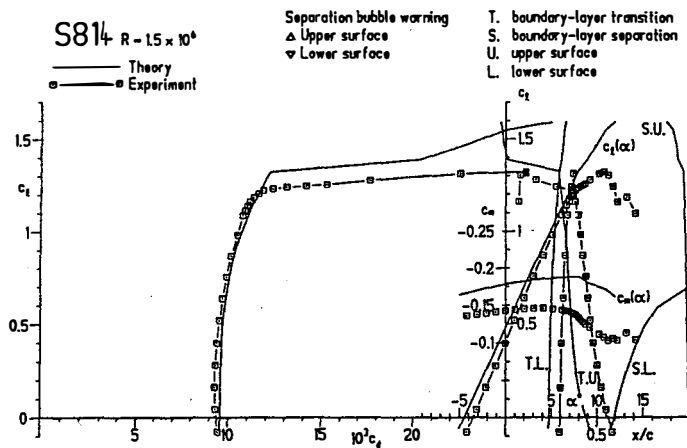


FIGURE 7. COMPARISON OF THEORETICAL AND EXPERIMENTAL SECTION CHARACTERISTICS WITH TRANSITION FREE (REYNOLDS NUMBER 1.5×10^6)

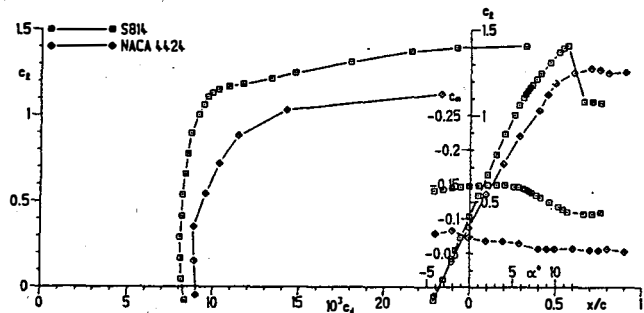


FIGURE 8. COMPARISON OF MEASURED SECTION CHARACTERISTICS OF S814 AND NACA 4424 AIRFOILS WITH TRANSITION FREE (REYNOLDS NUMBER 3.0×10^6)

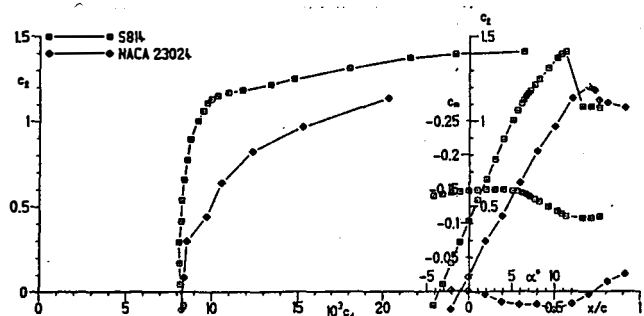


FIGURE 9. COMPARISON OF MEASURED SECTION CHARACTERISTICS OF S814 AND NACA 23024 AIRFOILS WITH TRANSITION FREE (REYNOLDS NUMBER 3.0×10^6)

moment coefficients than do the NACA airfoils. These comparisons confirm the achievement of the design objectives. In addition, the NACA 4424 and 23024 airfoils are known to suffer large reductions in $c_{l,max}$ due to roughness effects; whereas, the S814 airfoil was designed to minimize these effects.

CONCLUSIONS

The performance characteristics of a 24-percent-thick airfoil, the S814, for the root region of a horizontal-axis wind-turbine blade have been verified experimentally in the low-turbulence wind tunnel of the Delft University of Technology Low Speed Laboratory, The Netherlands. The two primary objectives of a high maximum lift coefficient, largely insensitive to leading-edge roughness, and low profile-drag coefficients have been achieved. The constraints on the zero-lift pitching-moment coefficient and the airfoil thickness have been satisfied. Comparisons of the theoretical and experimental results show good agreement with the exception of the maximum lift coefficient which is overpredicted. Comparisons with other airfoils illustrate the higher maximum lift coefficient and the lower profile-drag coefficients of the S814, thus confirming the achievement of the primary objectives.

ACKNOWLEDGEMENTS

The assistance of the staff of the Delft University of Technology Low Speed Laboratory is gratefully acknowledged. In particular, the meticulousness of Loek M. M. Boermans is sincerely appreciated. In addition, the diligence of Eric Wolfert Voet is recognized.

REFERENCES

- Eppler, R., 1994, "Airfoil Program System. User's Guide," c. '94.
- Somers, Dan M., 1988, "Design and Experimental Results for the S805 Airfoil," available from NREL.
- Somers, Dan M., 1989, "Design and Experimental Results for the S809 Airfoil," available from NREL.
- Somers, Dan M., 1992, "The S814 and S815 Airfoils," available from NREL.
- Somers, Dan M., 1994, "Design and Experimental Results for the S814 Airfoil," available from NREL.
- Braslow, Albert L., et al., 1958, "Simplified Method for Determination of Critical Height of Distributed Roughness Particles for Boundary-Layer Transition at Mach Numbers From 0 to 5," NACA TN 4363.
- Tangler, J. L., et al., 1990, "Atmospheric Performance of the Special Purpose SERI Thin-Airfoil Family: Final Results," European Wind Energy Conference, Madrid, Spain.
- Quast, Armin, 1987, "Detection of Transition by Infrared Image Technique, ICIASF '87 Record, pp.125-133.
- Abbott, Ira. H., et al., 1945, "Summary of Airfoil Data," NACA Rep. 824.